

## Article

# Developing a Model Based on the Radial Basis Function to Predict the Compressive Strength of Concrete Containing Fly Ash

Abdulilah Mohammad Mayet <sup>1</sup>, Ali Awadh Al-Qahtani <sup>1</sup>, Ramy Mohammed Aiesh Qaisi <sup>2</sup>, Ijaz Ahmad <sup>3</sup>, Hala H. Alhashim <sup>4</sup> and Ehsan Eftekhari-Zadeh <sup>5,\*</sup>

<sup>1</sup> Electrical Engineering Department, King Khalid University, Abha 61411, Saudi Arabia

<sup>2</sup> Department of Electrical and Electronic Engineering, College of Engineering, University of Jeddah, Jeddah 21589, Saudi Arabia

<sup>3</sup> Shenzhen College of Advanced Technology, University of Chinese Academy of Sciences (UCAS), Shenzhen 518055, China

<sup>4</sup> Department of Physics, College of Science, Imam Abdulrahman Bin Faisal University, P.O. Box 1982, Dammam 31441, Saudi Arabia

<sup>5</sup> Institute of Optics and Quantum Electronics, Friedrich Schiller University Jena, Max-Wien-Platz 1, 07743 Jena, Germany

\* Correspondence: e.eftekhari-zadeh@uni-jena.de

**Abstract:** A supplemental pozzolanic material such as fly ash may result in a reduction in the concrete's adverse environmental effect by reducing the discharge of carbon dioxide throughout the cement production procedure. This pozzolanic material also enhances the mechanical characteristics as well as the durability of concrete material. Considering the boundless passion for utilizing fly ash and conducting extensive research studies, the extent to which this supplement can be added to concrete has a limitation equal to almost one-third of cement material's weight. In the current study, a model based on the Radial Basis Function (RBF) is developed to estimate the compressive strength of concrete containing various amounts of fly ash at any arbitrary age. Having parameters used as inputs in ANN modeling such as concrete additives and characteristics of fly ash, the output was compressive strength. It was concluded that the estimated results agree well with the experimental measurements with an MSE of 0.0012 for the compressive strength. Simple and practical equations are proposed to present a simple means to determine the compressive strength of fly ash-based concrete.

**Keywords:** compressive strength; fly ash; radial basis function; estimation



**Citation:** Mayet, A.M.; Al-Qahtani, A.A.; Qaisi, R.M.A.; Ahmad, I.; Alhashim, H.H.; Eftekhari-Zadeh, E. Developing a Model Based on the Radial Basis Function to Predict the Compressive Strength of Concrete Containing Fly Ash. *Buildings* **2022**, *12*, 1743. <https://doi.org/10.3390/buildings12101743>

Academic Editors: Guoming Liu and Ben Li

Received: 21 September 2022

Accepted: 13 October 2022

Published: 19 October 2022

**Publisher's Note:** MDPI stays neutral with regard to jurisdictional claims in published maps and institutional affiliations.



**Copyright:** © 2022 by the authors. Licensee MDPI, Basel, Switzerland. This article is an open access article distributed under the terms and conditions of the Creative Commons Attribution (CC BY) license (<https://creativecommons.org/licenses/by/4.0/>).

## 1. Introduction

The mechanical performance and engineering properties of concrete can be enhanced by using mineral admixtures that have pozzolanic activity [1]. A sharp increase in the application of mineral admixtures can be observed owing to environmental and economic considerations. Cement with pozzolan leads to denser calcium silicate hydrate (C-S-H) and consequently less permeability and high compressive strength. Thus, awareness of the pozzolanic reactions development is important for its proper utilization and optimization when dealing with active admixtures [2]. In recent years, there has been an increasing interest in determining the cementing efficiency factor, which is defined as the impact of an admixture on improving a specific characteristic respecting the ratio of water to cement or the amount of cement in a mixture, and identification of influencing factors of a mineral admixture [3,4].

Fly ash categorized as Class C (higher calcium content) or Class F is a by-product of power generation plants, and it consists mainly of ferric oxide (Fe<sub>2</sub>O<sub>3</sub>), silicon dioxide

(SiO<sub>2</sub>), aluminum oxide (Al<sub>2</sub>O<sub>3</sub>) and calcium oxide (CaO) and some impurities [5]. The presence of SiO<sub>2</sub> and Al<sub>2</sub>O<sub>3</sub> is the main reason for fly ash's pozzolanic activity. The additional calcium aluminate hydrate (C-A-H) and C-S-H are important in making denser concrete paste, resulting in better durability and enhanced compressive strength formed by reacting with calcium hydroxide during cement hydration [6,7]. The presence of SiO<sub>2</sub> and Al<sub>2</sub>O<sub>3</sub> is the main reason that accounts for the pozzolanic reaction of the fly ash. On the other hand, concrete containing fly ash has the ability to show further particle packing and dense matrix due to its spherical particles, which produce the ball bearing effect [8,9]. Therefore, several remarkable results have been reported on the implementation of fly ash in concrete [10]. The advantages of fly ash utilization in concrete include improved workability, reduced hydration heat and thermal cracking in concrete at early ages, and enhanced mechanical as well as durability properties of concrete, especially at later ages [11–14].

This paper aims to present a simple and reliable empirical equation to predict the mechanical characteristics of concrete containing fly ash. For this purpose, three RBF networks were used. Recently, computational and numerical calculations as well as Digital Signal Processing (DSP), especially RBF as a very powerful mathematical tool, have wide application in different aspects of electrical engineering [15–20], civil engineering [21–23], mineral engineering [24,25], instrumentation and control engineering [26–28], nanoelectronic [29–31] and chemical and petrochemical engineering [32–38] problems. In this study, the same method is utilized. The number of hidden layers and neurons were calculated, and the RBF network was learned from previous samples using 1025 experimental specimens containing fly ash for compressive strength. The factors influencing the compression of fly ash concrete, namely the cement content (C), the amount of water (W), the level of fly ash replacement (FA), the amount of coarse aggregate (G), the amount of fine aggregate (S), the amount of SiO<sub>2</sub> (Si) in fly ash, and age (Age) were considered as inputs of the neural network, and the compressive strength was considered as the output. The inputs were selected in such a way that the impact of both physical and chemical parameters as well as the age of specimens on the mechanical characteristics of concrete could be contemplated. The results were juxtaposed with the experimental outcomes, and the error rate was dictated. In addition, simple empirical formulae are suggested to estimate the compressive strength of fly ash-based concrete. In the current study, several approaches for the practical utilization of RBF networks in the engineering field are proposed.

## 2. Radial Basis Function

Simplifying the models to use along with increasing the accuracy of outcomes using complex natural systems including a considerable number of inputs are the advantages of neural networks application [39]. Several uncomplicated operating elements that work in parallel are the basis of neural networks [40]. These networks are data supervisor models that are stimulated by mankind's brain [41,42]. It is practicable to build an artificial structure in compliance with natural networks and regulate the relation between its constituents by modifying the merits of each connection as well as the weight of the connection. Following modifying or training the artificial neural network, applying a particular input leads to a particular outcome. The foremost essential section of the learning procedure of the network is minimizing the error. This may be accomplished by replacing the weight throughout the training procedure and continuing until the error function, such as mean square error (MSE), is less than a particular amount. The MSE is calculated as follows:

$$MSE = \frac{1}{N} \sum_{i=1}^N (y_i - \hat{y}_i)^2 \quad (1)$$

where  $N$  stands for the number of samples, and  $y_i$  and  $\hat{y}_i$  are the experimental results and predicted outcomes of the proposed network, respectively. The challenge of the learning procedure in a network is regarding estimating the weights that lead to less MSE. In most artificial networks, the number of weights is vast, and therefore, they cannot be found

directly. Weight determination using a trial procedure has a computational cost. A Radial Basis Function (RBF) network is a sort of artificial neural network utilizing radial basis functions as an activation function of hidden layers. The most important application of this network is curve fitting in high-dimensional spaces [43,44]. In the proposed RBF network, the multi-variable functions are estimated using linear mergers of expressions according to one uni-variate function. This uni-variate function is the radial basis function. The activation function of the hidden layer in an RBF network is “radbas”; thus, the outcome from the hidden layer’s  $m^{th}$  neuron can be expressed as:

$$y_m = e^{-\frac{\|x-v_m\|^2}{2\sigma_m^2}} \quad (2)$$

### 2.1. Dataset

An in-depth and conscientious survey of the literature was conducted to propose a model to predict the compressive strength of concrete containing fly ash at any arbitrary age and by considering the chemical content of fly ash. The collected database includes about 1025 cases with seven distinguished features. The most important features that are considered as the inputs of the proposed network are cement content (C), water content (W), fly ash (FA), coarse aggregate (G), fine aggregate (S), SiO<sub>2</sub> content of fly ash (Si), and age of the specimens (Age). The mechanical characteristic of fly ash-based concrete, namely the compressive strength, was contemplated as the outcome of the RBF prediction model. These features are utilized to train and test the RBF network. The distribution and histogram of the features are depicted in Figure 1. Table 1 shows statistical factors for the fly-ash-based concrete dataset.

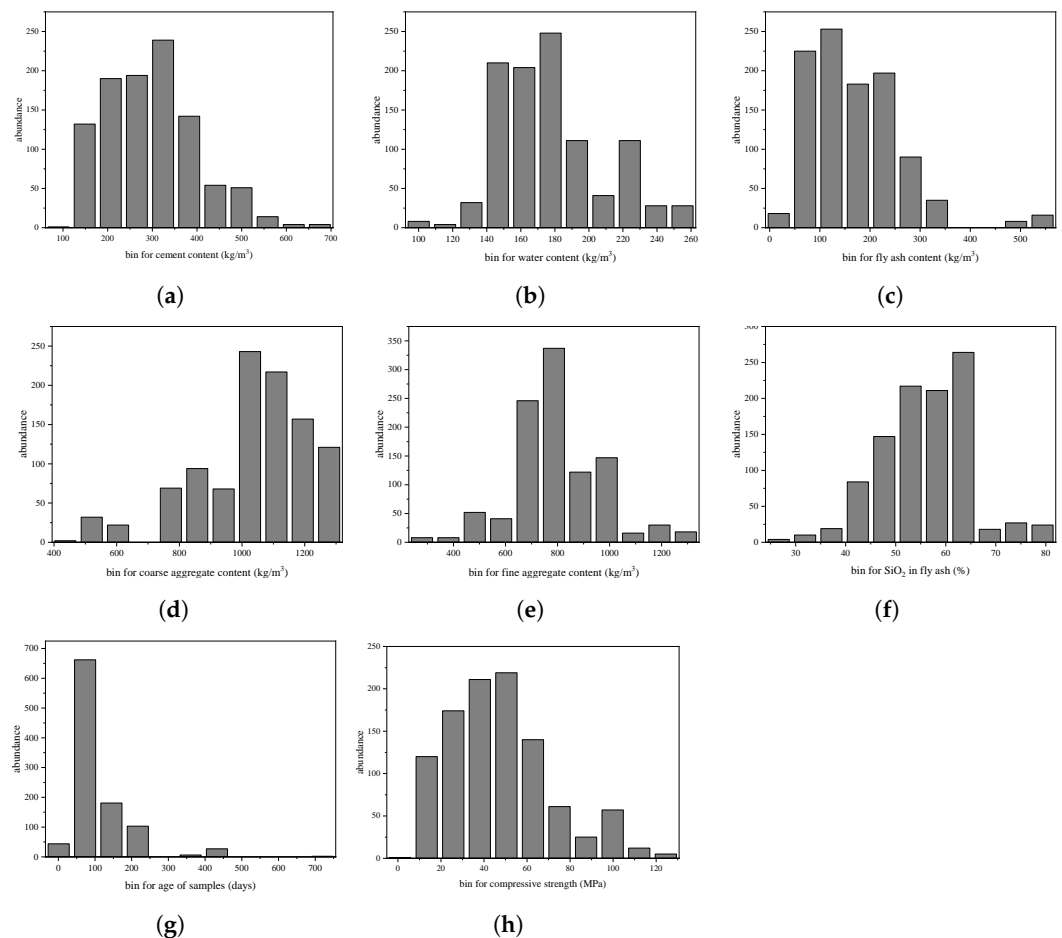


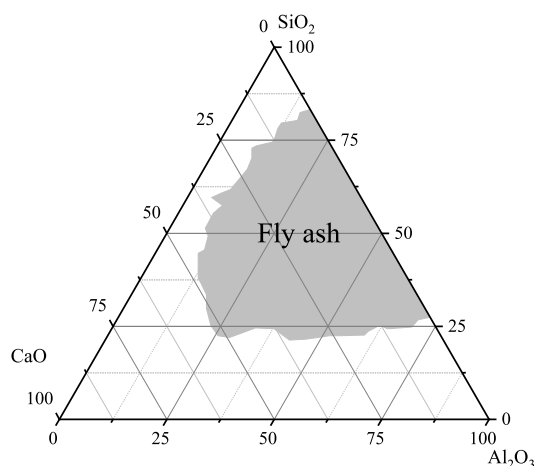
**Figure 1.** The data distribution of (a) cement, (b) water, (c) fly ash, (d) coarse aggregate, (e) fine aggregate, (f) SiO<sub>2</sub>, (g) age, and (h) compressive strength.

**Table 1.** Mathematical factors for the dataset of concrete containing fly ash.

Feature	Unit	Min	Max	Average	Standard Deviation
Cement	kg/m <sup>3</sup>	90	675	269.4	101.8
Water	kg/m <sup>3</sup>	100	255	169.9	30.4
Fly Ash	kg/m <sup>3</sup>	18	544	146.5	94.0
Coarse Aggregate	kg/m <sup>3</sup>	436	1278	989.8	178.8
Fine Aggregate	kg/m <sup>3</sup>	279	1293	751.9	169.7
SiO <sub>2</sub>	%	26.61	79.34	53.8	9.0
Age	days	1	720	63.3	81.9
Compressive Strength	MPa	1	124.5	40.9	24.0

### Materials and Experimental Design

The main objective of the current study is to develop a model based on the RBF function to estimate the compressive strength of concrete containing fly ash. The collected dataset contains various experimental works with different materials and methods. In order to reduce the effect of variation in the materials and methods, the chemical characteristic of fly ash is considered in the dataset. This pozzolanic material is categorized according to the Si content into two types, i.e., Class F and Class C, based on ASTM C 618 [45]. Class F fly ash contains more than 70% of four critical constituents, i.e., SiO<sub>2</sub>, CaO, Fe<sub>2</sub>O<sub>3</sub>, and Al<sub>2</sub>O<sub>3</sub>, while Class C has amounts between 50 and 70% [46,47]. Bituminous coal and old anthracite, which encompasses less than 7% CaO are the main sources of generation of Class F fly ash [48,49]. On the other hand, burning coal lignite or younger sub-bituminous that have specific properties of self-cementing are the main reasons for creating Class C fly ash [50]. In this study, the variation of SiO<sub>2</sub> content is from 26.6% to 79.3% in different previous experimental tests. The variation of the chemical composition for the entire fly ash material in the dataset is depicted in Figure 2. It is worth noting that due to the diversity of the samples' sizes and mold used to measure the compressive strength, during the construction of the network, the compressive strengths were converted to a cylindrical standard mold using the conversion factors reported by Elwell and Fu [51,52].

**Figure 2.** The variation of the chemical composition of fly ash material in the dataset.

### 2.2. Modeling the Network

In common, network modeling is the strategy of duplicating the real-world problems using mathematical functions [52–54]. It is principal to reform the network's arrangement in terms of the number of neurons to simultaneously provide a light weight and high quality at the same time. Due to the truth that there is no connection between the numbers of hidden layers and the numbers of neurons, the number of optimal hidden layers and neurons was calculated with trial and error. In the RBF network, the centers are selected

randomly, and then, the spread for the RBF function using the normalization method can be computed; after that, weights are computed by means of the pseudo-inverse method. Different configurations with various spreads and numbers of neurons in the hidden layer have been evaluated, and the high reasonable configuration with the lowest error rate was picked as the proposed RBF network. It was concluded that the RBF network having 15 neurons with a spread of 1 in one hidden layer for the  $f_c$  has the most reasonable performance. The configuration of the proposed RBF network is shown schematically in Figure 3. The database parameters are normalized in the range of 0 to 1 in a linear pattern to speed up the training procedure. This linear transformation preserves all the relationships of the initial database [41,55].

The aforementioned approach randomly divided the input data into two sections, 80% for the train and 20% for the test. PURELIN (Equation (3)) is considered as the activation function in the output layer. In the training process, the spread of radial basis functions (i.e.,  $\sigma$  in Equation (2)) was considered 1, and the MSE goal was considered 0. The training procedure will be completed whenever the desired performance of the network was achieved.

$$y = \text{purlin}(x) = x \quad (3)$$

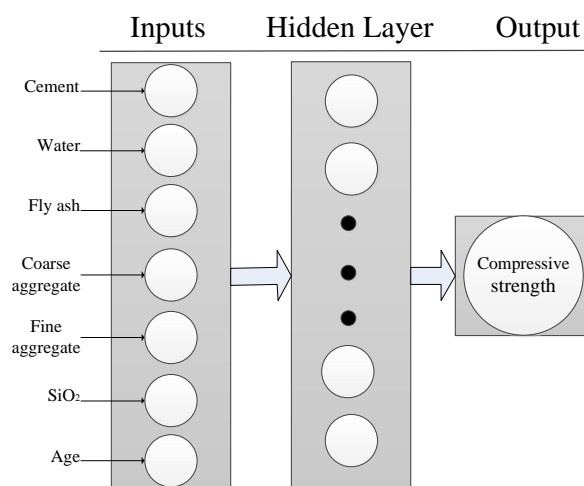


**Figure 3.** The configuration of the RBF network.

### Network Performance

Estimation of the mechanical characteristics of concrete including fly ash is achievable when the network is judiciously learned from available data. Furthermore, the compound interaction between the input factors and their impacts on output can be computed. The networks' performance to estimate the compressive strength is shown in Figure 4. As can be seen, the network is able to predict the results with suitable accuracy and performance. A critical challenge is selecting a suitable RBF configuration with a reasonable error without any underfitting or overfitting. The former indicates that the training model is simple and is not able to learn the relation between data [56,57], while the latter implies that the model is convoluted and the network memorizes the training dataset with limited ability in generalization [58,59]. In these conditions, due to the inaccurate learning procedure, the network is not able to generalize the unseen data. One good way to escape such a problem is using the early stopping procedure [58,60]. Moreover, as the MSE for test data reaches a constant value at a higher number of neurons, it indicates the proposed network is out of the risk for overfitting and underfitting [61]. In other words, an increase in the number of neurons may not result in an increase or a reduction in the MSE of the network. Therefore, one may be sure that the network is not stuck in the local minimum [57,62,63]. In addition, the difference between the MSE of test and train data is relatively low, which further indicates that there is not any overfitting in the network. Furthermore, by searching for a suitable configuration, a passive scheme of overfitting control is implemented. This

method searches for a suitable configuration of the network before training, which is called the hyper-parameter optimization technique or model selection approaches [57,58].

The condition of the prediction as a consequence of the coefficient of determination,  $R$ , in the network for all data is demonstrated in Figure 5, showing the interconnection between the RBF results and the experimental outcomes. Moreover, in Figure 5b, the comparison of the experimental results, i.e., targets, and RBF network outcomes, i.e., outputs, along with the corresponding errors is shown. As can be seen, the RBF network is able to predict the compressive strength of concrete containing fly ash at any age with reasonable accuracy. The proposed network can predict the compressive strength in a wide range from 1 MPa at 1-day age to more than 120 MPa. As can be noticed, the compressive strength of 1 MPa is very low, and it is related to the early-age strength, almost at the age of 1 day. However, the amount of error for the prediction of the compressive strength at early ages is relatively high. Figure 6 indicates the distribution of the estimation error for the proposed RBF-based network. As it is obvious, nearly half of the data was predicted using the proposed network with an error range of 5%, while more than 73% of the data, i.e., almost 750 samples, have an error of less than 10%. This demonstrates the accuracy of the proposed network and indicates a verification for further analysis of unseen data.

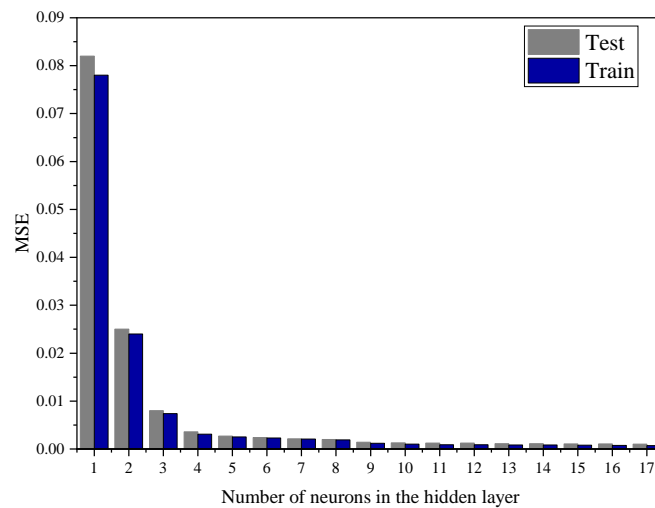


**Figure 4.** The performance of the network in predicting the compressive strength.

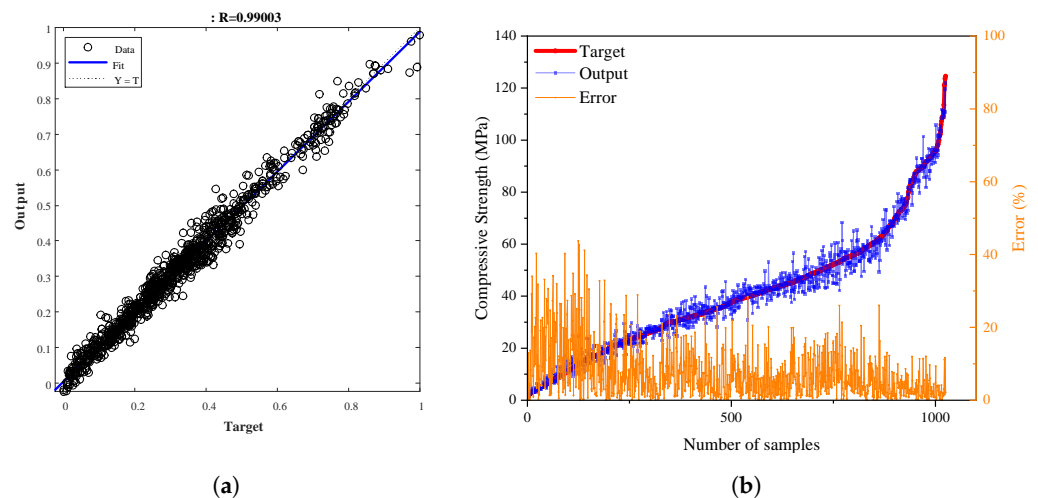


**Figure 5.** (a) The regression of the proposed networks, (b) comparison of the targets and outputs along with the corresponding error.

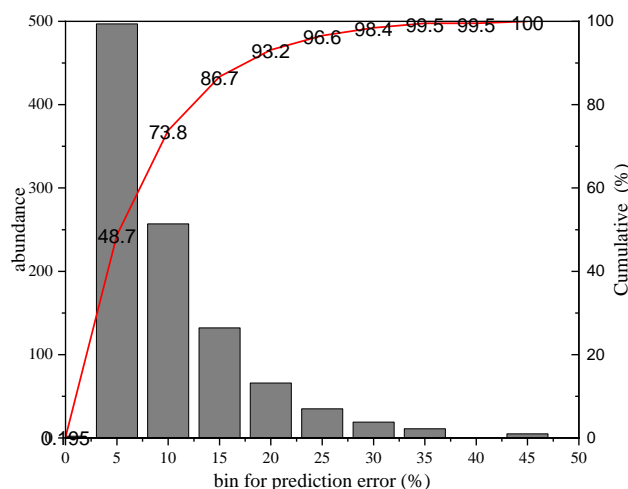


Figure 6. The distribution of the prediction error for the proposed network.

In order to show the precision of the network outputs in terms of statistical measures, four statistical error metrics such as correlation coefficient ( $R^2$ ), Nash–Sutcliffe efficiency (NSE) coefficient, root mean square error (RMSE), and mean absolute percentage error (MAPE) were used to comprehensively compare the outcomes of RBF network and experimental data. These statistical error indicators can be calculated by equations in Equation (4). These statistical metrics according to all data points obtained from the RBF networks are listed in Table 2. The statistical metrics listed in Table 2 indicate that the predicted compressive strength using the RBF network was very close to the experimental outcomes. This additionally verifies the eligibility of the proposed RBF model.

$$\begin{aligned}
 RMSE &= \sqrt{\frac{\sum(P - E)^2}{N}} & NSE &= 1 - \frac{\sum(P - E)^2}{\sum(\bar{E} - E)^2} \\
 MAPE &= \frac{100}{N} \sum \left| \frac{\bar{E} - P}{E} \right| & R &= \frac{\sum(P - \bar{P})(E - \bar{E})}{\sqrt{\sum(P - \bar{P})^2} \sqrt{\sum(E - \bar{E})^2}}
 \end{aligned}
 \tag{4}$$

where  $E$  and  $P$  are the experimental and predicted values, and the  $\bar{E}$  and  $\bar{P}$  factors are the mean values for the experimental and the predicted results, respectively.

Table 2. MSE, RMSE, NSE,  $R^2$  for the entire dataset in the RBF network.

Output of the Network	RBF Performance					
	MSE	RMSE	MAE	MAPE	NSE	$R^2$
Compressive strength	0.0012	0.034	0.022	13.85	0.974	0.990

### 2.3. Evaluation the Sensitivity of the RBF Network

In an artificial neural network, the neuron’s weight shows the importance of that neuron. In other words, the effectiveness and importance of each input feature can be determined using Garson’s factor [64]. For an RBF network with one hidden layer, the equation can be written as follows:

$$Q_{ik} = \frac{\sum_{j=1}^L \left( \frac{w_{ij}}{\sum_{r=1}^N w_{rj}} v_{jk} \right)}{\sum_{i=1}^N \left( \sum_{j=1}^L \frac{w_{ij}}{\sum_{r=1}^N w_{rj}} v_{jk} \right)}
 \tag{5}$$

where  $\sum_{r=1}^N w_{rj}$  is the summation of the weights of connection between the  $N$  input neurons and the hidden neuron  $j$ , and  $v_{jk}$  is the weight of connection between the hidden

neuron  $j$  and the output neuron  $k$  [54]. Evaluation of the sensitivity of the RBF network is demonstrated in Figure 7.

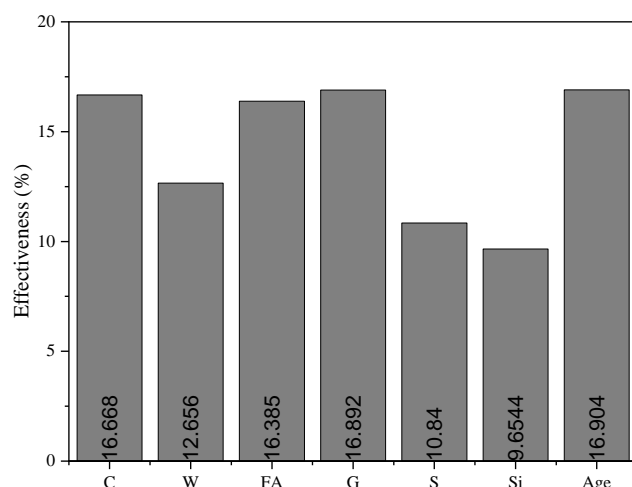


**Figure 7.** Relative importance of the input factors in the RBF network.

As can be seen, nearly all the factors have a similar engagement in calculating the compressive strength of concrete containing fly ash. On this subject, it may be said that no unrelated, excess, or irrelevant factors have been embraced in the proposed network. By ruling out the extra factors in the estimation procedure, the degradation of the training approach is prevented, which leads to further accuracy of the estimation [65,66]. The most important features that have a remarkable impact on improving the compressive strength of the concrete containing fly ash are cement content, coarse aggregate, the presence of fly ash, and the age of the concrete samples. Conversely, the  $\text{SiO}_2$  content of fly ash has a relatively insignificant impact on the compressive strength. However, since the fly ash-based concrete's compressive strength is affected by the  $\text{SiO}_2$  content of fly ash, these parameters remain in the proposed network [67,68]. Generally, the existence of  $\text{SiO}_2$  in the concrete mixture improves the mechanical properties, e.g., rise in the compressive strength, by forming silica–oxygen bonds; which are stronger compared to the bonds of aluminum–oxygen and silica–oxygen–aluminum [69].

### 3. Results

Influential computational approaches have been implemented to resolve sophisticated problems, particularly in the engineering field in recent years [70,71]. This novel method can be implemented for simulating, evaluating, and estimating with reasonable precision. The precision of the network to generate new outcomes according to the previous input factors, i.e., generalization, should be computed based on the proven facts or theoretical results. Generalization of the RBF network is the ability to handle unseen data and to produce results which are difficult or even impossible to obtain.

Since the aim of this paper is to predict the compressive strength of concrete containing fly ash at any arbitrary age, the fly ash percentages, age of specimens, and the  $\text{SiO}_2$  content of fly ash were considered as variables, and the variation of the compressive strength due to their changes was calculated. This evaluation is not out of the question, as the compressive strength of fly ash-based concrete as an essential factor to evaluate the quality of concrete is under the influence of fly ash's chemical specifications along with the age of concrete [68]. The presumed concrete mix design is summarized in Table 3. The water to binder ratio is assumed to be 0.28, and the fly ash replaces the cement in the concrete specimens up to 30% of cement weight. Fly ash takes action as a pozzolanic material in a concrete mixture containing a low replacement percentage. On the other hand, in the mixture with a higher replacement percentage, some part of fly ash takes part in the pozzolanic reaction, while the rest of the fly ash remains unchanged even after a long time of curing and acts as a

packing material [72]. Therefore, the amount of fly ash to be used in a concrete mixture is limited by American and British standards to 35% in structural concrete [73,74]. It is worth noting that the entire simulations have been completed in the absence of the experimentally investigated domain, which is only feasible using artificial intelligence methods.

**Table 3.** The presumed mix design of concrete.

Concrete Specimen	C (kg/m <sup>3</sup> )	W (kg/m <sup>3</sup> )	G (kg/m <sup>3</sup> )	S (kg/m <sup>3</sup> )	SiO <sub>2</sub> (%)	FA (kg/m <sup>3</sup> )	Age (days)
C40	500	140	1135	644	61.7	12.5–150	3–365

The amount of this pozzolanic material that should replace the cement in a concrete mixture for typical implementation to gain optimum results has not yet been evaluated. The disparity in the compressive strength versus the content of fly ash along with the age of specimens for various amounts of SiO<sub>2</sub> contents is shown in Figure 8. It is worth noting that the scale of the vertical axis in Figure 8 is logarithmic due to better presentation. Based on the results, it can be concluded that an increase in the fly ash replacement level has a positive effect on those fly ashes with a higher amount of SiO<sub>2</sub>, i.e., Class F fly ash. This observation is in accordance with the results of Sumer's experiments [75]. An increase in the age of concrete samples containing Class C fly ash may lead the variation of compressive strength to be independent of the fly ash replacement level. This trend can be attributed to the fact that the fly ash reaction with calcium hydroxide and water is time consuming [76]. Moreover, the utilization of Class C fly ash (with lower SiO<sub>2</sub> content) in concrete may result in a higher compressive strength in all ages compared with the implementation of Class F fly ash. The same results were obtained in experimental research of Uysal and Akyuncu [77]. In addition, concrete samples containing Class F fly ash with a high amount of SiO<sub>2</sub> have a relatively low compressive strength at early ages, even until 28 days, which can be seen in Figure 8c,d. This is in accordance with previous experimental research [75,78]. This behavior, which is correctly anticipated in the results of the proposed network, is because the disintegration process of glass materials in fly ash is time consuming. This reaction occurs in an alkaline environment with a pH value of more than 13. A reason for a rise in the alkalinity of the concrete mixture is that a specific amount of cement hydration occurs. Therefore, as it was shown in this section, the outcomes generated using the RBF network are in accordance with proven facts as well as experimental results. This may further verify the outcomes of the proposed network and by ensuring the accuracy of the results, some equations can be developed to predict the compressive strength of concrete containing fly ash at various ages.

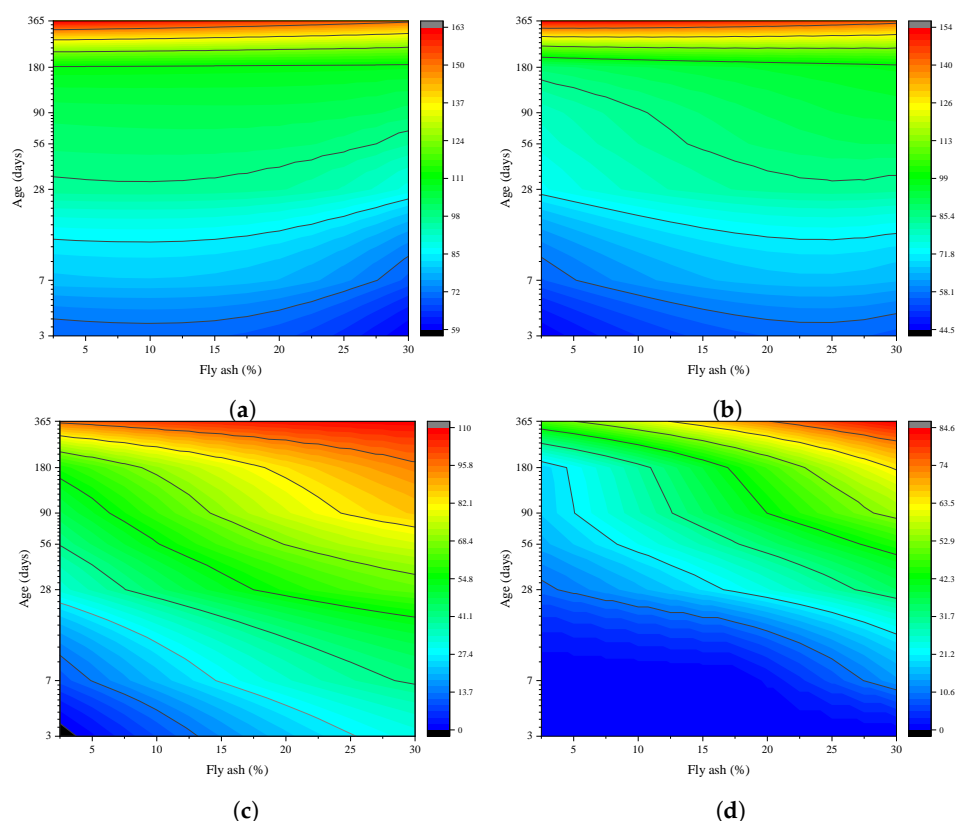


**Figure 8.** The trend of compressive strength variation versus the level of fly ash replacement for  $\text{SiO}_2$  content of (a) 40%, (b) 50%, (c) 60%, and (d) 70%.

#### *Development of Equations to Calculate the Compressive Strength of Concrete Containing Fly Ash*

The same contribution of the input factors on the compressive strength prediction, an appropriate match between the outcomes of the RBF network and the proven fact and experimental results, and the reasonable precision of outcomes of the RBF network allows the implementation of the RBF models to estimate the experimental outcomes and at the higher level proposed estimation equations. The equation benefits from the weights and biases of the RBF model to estimate the compressive strength of fly ash-based concrete at various ages for different types of fly ash. The limitation of using artificial intelligence in practical use may be reduced by developing empirical design charts and/or formulae. The proposed equation for anticipating the compressive strength of fly ash-based concrete was according to the conducted study by Leung et al. [79]. To develop an empirical equation, the most influential factor on the outcomes of the RBF network should be calculated.

Figure 7 shows that the age of the concrete samples has relatively more influence than the other factors. The variation of compressive strength versus the age of samples while the other factors put in their median value is determined, and a curve-fitting procedure is conducted on data to obtain the equation relating the compressive strength to the age of specimens. A similar plan of action was conducted for other neurons in the input layer, while the amount of cement is kept constant at its median. It is presumed that the disparity of the compressive strength with each factor is autonomous of the other factors and may be stated as Equation (6). In this formula, the compressive strength of concrete is determined based on the variation of specimen ages. A correction function has to be obtained for accounting for the impact of other input factors on the compressive strength. A line that fits best to the aforementioned curve and has the lowest MSE is calculated using the curve-fitting tool in MATLAB. The curve-fitting procedure is conducted in a way that a suitable balance between accuracy and simplicity is made. Therefore, most of the correction functions are in a simple format of mathematical equations. It is worth noting that the limitation of the proposed network is in the age of the specimens. In other words,

the proposed equations in this study are able to predict the compressive strength of concrete containing fly ash with an age of more than 7 days. However, this limitation does not exist in the RBF network.

$$\text{Compressive strength} = [C_c \times C_w \times C_{FA} \times C_G \times C_S \times C_{si}] \times \text{Age} \quad (6)$$

$$\text{Age} = 0.01125 \left( \frac{\text{Age}}{28} \right)^3 - 0.6227 \left( \frac{\text{Age}}{28} \right)^2 + 8.43 \left( \frac{\text{Age}}{28} \right) + 35.35 \quad (7)$$

After finishing the curve-fitting procedure, the formulae are derived to determine the compressive strength of concrete containing fly ash as the pozzolan. These formulae are summarized in Table 4. In order to show the accuracy of the proposed formula, the outcomes of the empirical approach are compared to experimental results. This comparison is demonstrated in Figure 9. The error distribution as percentage distinction within the experimental and predicted results are listed in Table 5. The mean square error and R coefficient of the proposed formula in anticipating the compressive strength of concrete are 0.0028 and 0.7848, respectively. The RBF network reached 93.7%, 96.8%, and 97.5% of samples in the error range of  $\pm 20\%$ ,  $\pm 30\%$ , and  $\pm 40\%$ , respectively. The proposed equation indicated a significant accuracy. The proposed equation is able to predict about 62.5% of the samples regarding the compressive strength with the  $\pm 20\%$  of error range, about 74.6% with the error range of  $\pm 30$ , and roughly 82% of samples with  $\pm 40\%$  the range of error. Although, due to the limitation of the proposed equation, almost 126 data were not used in the comparison. In other words, the number of data to be compared with the proposed equation is 899 samples. As can be seen, the proposed equation is easy to implement and also practical with reasonable accuracy.

**Table 4.** The equations for correcting the estimation of each output.

Correction Factor	Equation
$C_c$	$1.86 \left( \frac{C}{264} \right) - 0.72$
$C_w$	$3.046 \left( \frac{W}{163} \right)^2 - 8.67 \left( \frac{W}{163} \right) + 6.624$
$C_{FA}$	$0.6438 \left( \frac{F.A.}{128} \right) + 0.3562$
$C_G$	$0.1591 \left( \frac{G}{1017} \right) + 0.742$
$C_S$	$0.8549 \left( \frac{S}{743} \right)^2 - 1.189 \left( \frac{S}{743} \right) + 1.319$
$C_{si}$	$1.31 \left( \frac{Si}{55.3} \right)^2 - 2.408 \left( \frac{Si}{55.3} \right) + 2.098$

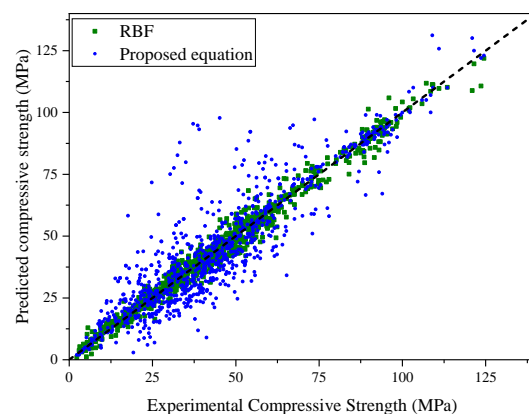


**Figure 9.** Comparison between experimental and predicted mechanical properties.

**Table 5.** Accuracy of suggested approaches and distribution of samples in the error range.

Compressive Strength	Approach	MSE	Determination Coefficient	Number and % of Data in Error Range		
				$\pm 20\%$	$\pm 40\%$	$\pm 60\%$
	RBF Network	0.0012	0.9900	955 (93.7%)	1020 (99.5%)	1025 (100%)
	Proposed equation	0.0028	0.7848	562 (62.5%)	671 (74.6%)	738 (82%)

#### 4. Conclusions

A large number of targets of the RBF network which correspond to the experimental data for the fly ash-based concrete were gathered. Seven distinguished affecting factors on the compressive strength of fly ash-based concrete—namely, cement, water, fly ash, coarse and fine aggregates, SiO<sub>2</sub> content of fly ash along with the age of specimens—were considered. A RBF network was developed to anticipate the compressive strength of concrete corresponding to the inputs. The inputs have the ability to consider all aspects of fly ash-based concrete in terms of physical and chemical composition. Moreover, the age of concrete as an important factor was considered. The high number of experimental samples along with considering the age of specimens make the proposed network a comprehensive and accurate model to predict a fundamental parameter such as compressive strength.

The results of the RBF network show an excellent accuracy in predicting the compressive strength with an MSE of 0.0012. On the other hand, about 94% of the simulated results were within  $\pm 20$  of the experimental compressive strength for the RBF network, demonstrating that the suggested RBF network was learned to generalize the information well. In addition, the RBF's prediction outcomes were scattered about the bisector, which demonstrates neither under-prediction nor over-prediction. Simple and practical formulae were obtained according to outcomes to simplify the practical implementation of the achieved results of the RBF network for anticipating the compressive strength of concrete containing fly ash. It was shown that the proposed formulae have a reasonable accuracy with an MSE of 0.0028 and the ability to predict more than 62% of the experimental compressive strength in the error range of  $\pm 20$ .

In the current study, only the compressive strength of concrete was considered as the output of the network, while the other parameters such as tensile strength and modulus of elasticity or durability properties were considered only if there was a sufficient amount of data available. Moreover, the effect of other supplementary cementitious materials—namely, Metakaolin, Zeolite, furnace slag, and so on—can be determined using the ability of an artificial neural network in estimating the results.

**Author Contributions:** Conceptualization, A.M.M., A.A.A.-Q., R.M.A.Q., I.A., H.H.A. and E.E.-Z.; methodology, A.M.M., A.A.A.-Q., R.M.A.Q., I.A., H.H.A. and E.E.-Z.; software, A.M.M., A.A.A.-Q., R.M.A.Q., I.A., H.H.A. and E.E.-Z.; validation, A.M.M., A.A.A.-Q., R.M.A.Q., I.A., H.H.A. and E.E.-Z.; formal analysis, A.M.M., A.A.A.-Q., R.M.A.Q., I.A., H.H.A. and E.E.-Z.; investigation, A.M.M., A.A.A.-Q., R.M.A.Q., I.A., H.H.A. and E.E.-Z.; resources, A.M.M., A.A.A.-Q., R.M.A.Q., I.A., H.H.A. and E.E.-Z.; data curation, A.M.M., A.A.A.-Q., R.M.A.Q., I.A., H.H.A. and E.E.-Z.; writing—original draft preparation, A.M.M., A.A.A.-Q., R.M.A.Q., I.A., H.H.A. and E.E.-Z.; writing—review and editing, A.M.M., A.A.A.-Q., R.M.A.Q., I.A., H.H.A. and E.E.-Z.; visualization, A.M.M., A.A.A.-Q., R.M.A.Q., I.A., H.H.A. and E.E.-Z.; supervision, A.M.M., A.A.A.-Q., R.M.A.Q., I.A., H.H.A. and E.E.-Z.; funding acquisition, A.M.M., A.A.A.-Q., R.M.A.Q., I.A., H.H.A. and E.E.-Z. All authors have read and agreed to the published version of the manuscript.

**Funding:** This work was supported by the Deanship of Scientific Research at King Khalid University (grant numbers RGP. 2/39/44). The authors acknowledge support from the German Research Foundation and the Open Access Publication Fund of the Thueringer Universitaets-und Landesbibliothek Jena Projekt-Nr. 433052568; the BMBF-Projekt 05P21SJFA2 Verbundprojekt 05P2021 (ErUM-FSP T05).

**Data Availability Statement:** The data presented in this study are available on request from the corresponding author.

**Conflicts of Interest:** The authors declare no conflict of interest.

### Abbreviations

The following abbreviations are used in this manuscript:

RBF	Radial Basis Function
ANN	Artificial Neural Network
MSE	Mean square error
C	Cement
W	Water
FA	Fly ash
G	Coarse aggregate
S	Fine aggregate
Si	SiO <sub>2</sub> content

### References

- Shi, T.; Liu, Y.; Zhang, Y.; Lan, Y.; Zhao, Q.; Zhao, Y.; Wang, H. Calcined attapulgite clay as supplementary cementing material: Thermal treatment, hydration activity and mechanical properties. *Int. J. Concr. Struct. Mater.* **2022**, *16*, 10. [[CrossRef](#)]
- Aponte, D.F.; Barra, M.; Vázquez, E. Durability and cementing efficiency of fly ash in concretes. *Constr. Build. Mater.* **2012**, *30*, 537–546. [[CrossRef](#)]
- Badogiannis, E.; Papadakis, V.; Chaniotakis, E.; Tsvivilis, S. Exploitation of poor Greek kaolins: Strength development of metakaolin concrete and evaluation by means of k-value. *Cem. Concr. Res.* **2004**, *34*, 1035–1041. [[CrossRef](#)]
- Farhangi, V.; Karakouzian, M. Effect of fiber reinforced polymer tubes filled with recycled materials and concrete on structural capacity of pile foundations. *Appl. Sci.* **2020**, *10*, 1554. [[CrossRef](#)]
- Oner, A.; Akyuz, S.; Yildiz, R. An experimental study on strength development of concrete containing fly ash and optimum usage of fly ash in concrete. *Cem. Concr. Res.* **2005**, *35*, 1165–1171. [[CrossRef](#)]
- Malvar, L.J.; Lenke, L.R. Efficiency of fly ash in mitigating alkali-silica reaction based on chemical composition. *ACI Mater. J.* **2006**, *103*, 319.
- Shaikh, F.U.A.; Supit, S.W. Chloride induced corrosion durability of high volume fly ash concretes containing nano particles. *Constr. Build. Mater.* **2015**, *99*, 208–225. [[CrossRef](#)]
- Ahmaruzzaman, M. A review on the utilization of fly ash. *Prog. Energy Combust. Sci.* **2010**, *36*, 327–363. [[CrossRef](#)]
- Daneshvar, K.; Moradi, M.; Ahmadi, K.; Hajiloo, H. Strengthening of corroded reinforced concrete slabs under multi-impact loading: Experimental results and numerical analysis. *Constr. Build. Mater.* **2021**, *284*, 122650. [[CrossRef](#)]
- Siddique, R. Effect of fine aggregate replacement with Class F fly ash on the mechanical properties of concrete. *Cem. Concr. Res.* **2003**, *33*, 539–547. [[CrossRef](#)]
- Hemalatha, T.; Ramaswamy, A. A review on fly ash characteristics—Towards promoting high volume utilization in developing sustainable concrete. *J. Clean. Prod.* **2017**, *147*, 546–559. [[CrossRef](#)]
- Salimi, J.; Ramezani-pour, A.M.; Moradi, M.J. Studying the effect of low reactivity metakaolin on free and restrained shrinkage of high performance concrete. *J. Build. Eng.* **2020**, *28*, 101053. [[CrossRef](#)]
- Aghayari, R.; Moradi, M. Improving the punching shear strength of RC slabs by FRP and steel sheets. *J. Rehabil. Civ. Eng.* **2016**, *4*, 1–17.
- Daneshvar, K.; Moradi, M.J.; Amooie, M.; Chen, S.; Mahdavi, G.; Hariri-Ardebili, M.A. Response of low-percentage FRC slabs under impact loading: Experimental, numerical, and soft computing methods. *Structures* **2020**, *27*, 975–988. [[CrossRef](#)]
- Lalbaksh, A.; Mohamadpour, G.; Roshani, S.; Ami, M.; Roshani, S.; Sayem, A.S.M.; Alibakhshikenari, M.; Koziel, S. Design of a compact planar transmission line for miniaturized rat-race coupler with harmonics suppression. *IEEE Access* **2021**, *9*, 129207–129217. [[CrossRef](#)]
- Hookari, M.; Roshani, S.; Roshani, S. High-efficiency balanced power amplifier using miniaturized harmonics suppressed coupler. *Int. J. RF Microw. Comput. Aided Eng.* **2020**, *30*, e22252. [[CrossRef](#)]
- Lotfi, S.; Roshani, S.; Roshani, S.; Gilan, M.S. Wilkinson power divider with band-pass filtering response and harmonics suppression using open and short stubs. *Frequenz* **2020**, *74*, 169–176. [[CrossRef](#)]
- Jamshidi, M.; Siahkamari, H.; Roshani, S.; Roshani, S. A compact Gysel power divider design using U-shaped and T-shaped resonators with harmonics suppression. *Electromagnetics* **2019**, *39*, 491–504. [[CrossRef](#)]
- Roshani, S.; Jamshidi, M.B.; Mohebi, F.; Roshani, S. Design and modeling of a compact power divider with squared resonators using artificial intelligence. *Wirel. Pers. Commun.* **2021**, *117*, 2085–2096. [[CrossRef](#)]
- Roshani, S.; Azizian, J.; Roshani, S.; Jamshidi, M.B.; Parandini, F. Design of a miniaturized branch line microstrip coupler with a simple structure using artificial neural network. *Frequenz* **2022**, *76*, 255–263. [[CrossRef](#)]
- Daneshvar, K.; Moradi, M.; Khaleghi, M.; Rezaei, M.; Farhangi, V.; Hajiloo, H. Effects of impact loads on heated-and-cooled reinforced concrete slabs. *J. Build. Eng.* **2022**, *61*, 105328. [[CrossRef](#)]

22. Baldo, N.; Manthos, E.; Pasetto, M. Analysis of the mechanical behaviour of asphalt concretes using artificial neural networks. *Adv. Civ. Eng.* **2018**, *2018*, 1650945. [[CrossRef](#)]
23. Ramzi, S.; Moradi, M.J.; Hajiloo, H. Artificial Neural Network in Predicting the Residual Compressive Strength of Concrete after High Temperatures. Available at SSRN 4222748. [[CrossRef](#)]
24. Liu, Y.; Zhang, Z.; Liu, X.; Wang, L.; Xia, X. Efficient image segmentation based on deep learning for mineral image classification. *Adv. Powder Technol.* **2021**, *32*, 3885–3903. [[CrossRef](#)]
25. Liu, Y.; Zhang, Z.; Liu, X.; Wang, L.; Xia, X. Ore image classification based on small deep learning model: Evaluation and optimization of model depth, model structure and data size. *Miner. Eng.* **2021**, *172*, 107020. [[CrossRef](#)]
26. Zych, M.; Petryka, L.; Kępiński, J.; Hanus, R.; Bujak, T.; Puskarczyk, E. Radioisotope investigations of compound two-phase flows in an open channel. *Flow Meas. Instrum.* **2014**, *35*, 11–15. [[CrossRef](#)]
27. Zych, M.; Hanus, R.; Wilk, B.; Petryka, L.; Świsulski, D. Comparison of noise reduction methods in radiometric correlation measurements of two-phase liquid-gas flows. *Measurement* **2018**, *129*, 288–295. [[CrossRef](#)]
28. Golijanek-Jędrzejczyk, A.; Mrowiec, A.; Hanus, R.; Zych, M.; Świsulski, D. Uncertainty of mass flow measurement using centric and eccentric orifice for Reynolds number in the range. *Measurement* **2020**, *160*, 107851. [[CrossRef](#)]
29. Mayet, A.; Smith, C.E.; Hussain, M.M. Energy reversible switching from amorphous metal based nanoelectromechanical switch. In Proceedings of the 2013 13th IEEE International Conference on Nanotechnology (IEEE-NANO 2013), Beijing, China, 5–8 August 2013; IEEE: Piscataway, NJ, USA, 2013; pp. 366–369.
30. Shukla, N.K.; Mayet, A.M.; Vats, A.; Aggarwal, M.; Raja, R.K.; Verma, R.; Muqet, M.A. High speed integrated RF-VLC data communication system: Performance constraints and capacity considerations. *Phys. Commun.* **2022**, *50*, 101492. [[CrossRef](#)]
31. Mayet, A.M.; Hussain, A.M.; Hussain, M.M. Three-terminal nanoelectromechanical switch based on tungsten nitride—An amorphous metallic material. *Nanotechnology* **2015**, *27*, 035202. [[CrossRef](#)]
32. Khaibullina, K. Technology to remove asphaltene, resin and paraffin deposits in wells using organic solvents. In Proceedings of the SPE Annual Technical Conference and Exhibition, Dubai, United Arab Emirates, 26–28 September 2016.
33. Khaibullina, K.S.; Korobov, G.Y.; Lekomtsev, A. Development of an asphalt-resin-paraffin deposits inhibitor and substantiation of the technological parameters of its injection into the bottom-hole formation zone. *Period. Tche Quim* **2020**, *17*, 769–781. [[CrossRef](#)]
34. Khaibullina, K.S.; Sagirova, L.R.; Sandyga, M.S. Substantiation and selection of an inhibitor for preventing the formation of asphalt-resin-paraffin deposits. *Period. Tche Quim.* **2020**, *17*, 541–551. [[CrossRef](#)]
35. Tikhomirova, E.; Sagirova, L.; Khaibullina, K.S. A review on methods of oil saturation modelling using IRAP RMS. In *IOP Conference Series: Earth and Environmental Science*; IOP Publishing: Bristol, UK, 2019; Volume 378, p. 012075.
36. Mayet, A.M.; Alizadeh, S.M.; Nurgalieva, K.S.; Hanus, R.; Nazemi, E.; Narozhnyy, I.M. Extraction of Time-Domain Characteristics and Selection of Effective Features Using Correlation Analysis to Increase the Accuracy of Petroleum Fluid Monitoring Systems. *Energies* **2022**, *15*, 1986. [[CrossRef](#)]
37. Mayet, A.M.; Alizadeh, S.M.; Kakarash, Z.A.; Al-Qahtani, A.A.; Alanazi, A.K.; Alhashimi, H.H.; Eftekhari-Zadeh, E.; Nazemi, E. Introducing a Precise System for Determining Volume Percentages Independent of Scale Thickness and Type of Flow Regime. *Mathematics* **2022**, *10*, 1770. [[CrossRef](#)]
38. Hanus, R.; Zych, M.; Golijanek-Jędrzejczyk, A. Investigation of Liquid–Gas Flow in a Horizontal Pipeline Using Gamma-Ray Technique and Modified Cross-Correlation. *Energies* **2022**, *15*, 5848. [[CrossRef](#)]
39. Dabiri, H.; Farhangi, V.; Moradi, M.J.; Zadehmohamad, M.; Karakouzian, M. Applications of Decision Tree and Random Forest as Tree-Based Machine Learning Techniques for Analyzing the Ultimate Strain of Spliced and Non-Spliced Reinforcement Bars. *Appl. Sci.* **2022**, *12*, 4851. [[CrossRef](#)]
40. Daneshvar, K.; Moradi, M.J.; Ahmadi, K.; Mahdavi, G.; Hariri-Ardebili, M.A. Dynamic behavior of corroded RC slabs with macro-level stochastic finite element simulations. *Eng. Struct.* **2021**, *239*, 112056. [[CrossRef](#)]
41. Moradi, M.J.; Roshani, M.M.; Shabani, A.; Kioumars, M. Prediction of the Load-Bearing Behavior of SPSW with Rectangular Opening by RBF Network. *Appl. Sci.* **2020**, *10*, 1185. [[CrossRef](#)]
42. Khaleghi, M.; Salimi, J.; Farhangi, V.; Moradi, M.J.; Karakouzian, M. Evaluating the behaviour of centrally perforated unreinforced masonry walls: Applications of numerical analysis, machine learning, and stochastic methods. *Ain Shams Eng. J.* **2022**, *13*, 101631. [[CrossRef](#)]
43. Roshani, M.; Phan, G.T.; Ali, P.J.M.; Roshani, G.H.; Hanus, R.; Duong, T.; Corniani, E.; Nazemi, E.; Kalmoun, E.M. Evaluation of flow pattern recognition and void fraction measurement in two phase flow independent of oil pipeline’s scale layer thickness. *Alex. Eng. J.* **2021**, *60*, 1955–1966. [[CrossRef](#)]
44. Akhaveissy, A.; Daneshvar, K.; Ghazi-Nader, D.; Amooie, M.; Moradi, M.J. Numerical Study on Seismic Behavior of Composite Shear Walls with Steel-Encased Profiles Subjected to Different Axial Load. *Pract. Period. Struct. Des. Constr.* **2021**, *26*, 04021034. [[CrossRef](#)]
45. ASTM C-618; American Society for Testing and Materials, ASTM Specification for Fly Ash and Raw or Calcined Natural Pozzolan for use as a Mineral Admixture in Portland Cement Concrete, Designation C618. ASTM International: Conshohocken, PA, USA, 2002.
46. Baldo, N.; Rondinella, F.; Daneluz, F.; Pasetto, M. Foamed Bitumen Mixtures for Road Construction Made with 100% Waste Materials: A Laboratory Study. *Sustainability* **2022**, *14*, 6056. [[CrossRef](#)]

47. Amran, M.; Fediuk, R.; Murali, G.; Avudaiappan, S.; Ozbakkaloglu, T.; Vatin, N.; Karelina, M.; Klyuev, S.; Gholampour, A. Fly ash-based eco-efficient concretes: A comprehensive review of the short-term properties. *Materials* **2021**, *14*, 4264. [[CrossRef](#)] [[PubMed](#)]
48. Pasetto, M.; Baldo, N. Laboratory investigation on foamed bitumen bound mixtures made with steel slag, foundry sand, bottom ash and reclaimed asphalt pavement. *Road Mater. Pavement Des.* **2012**, *13*, 691–712. [[CrossRef](#)]
49. Salih, M.A.; Ali, A.A.A.; Farzadnia, N. Characterization of mechanical and microstructural properties of palm oil fuel ash geopolymer cement paste. *Constr. Build. Mater.* **2014**, *65*, 592–603. [[CrossRef](#)]
50. Mahlia, T.; Abdulmuin, M.; Alamsyah, T.; Mukhlisien, D. An alternative energy source from palm wastes industry for Malaysia and Indonesia. *Energy Convers. Manag.* **2001**, *42*, 2109–2118. [[CrossRef](#)]
51. Elwell, D.J.; Fu, G. *Compression Testing of Concrete: Cylinders vs. Cubes*; Technical Report; State Department of Transportation: New York, NY, USA, 1995.
52. Moradi, M.; Khaleghi, M.; Salimi, J.; Farhangi, V.; Ramezani-pour, A. Predicting the compressive strength of concrete containing metakaolin with different properties using ANN. *Measurement* **2021**, *183*, 109790. [[CrossRef](#)]
53. Zadeh, E.E.; Feghhi, S.; Roshani, G.; Rezaei, A. Application of artificial neural network in precise prediction of cement elements percentages based on the neutron activation analysis. *Eur. Phys. J. Plus* **2016**, *131*, 167. [[CrossRef](#)]
54. Moradi, M.; Daneshvar, K.; Ghazi-Nader, D.; Hajiloo, H. The prediction of fire performance of concrete-filled steel tubes (CFST) using artificial neural network. *Thin-Walled Struct.* **2021**, *161*, 107499. [[CrossRef](#)]
55. Khaleghi, M.; Salimi, J.; Farhangi, V.; Moradi, M.J.; Karakouzian, M. Application of artificial neural network to predict load bearing capacity and stiffness of perforated masonry walls. *CivilEng* **2021**, *2*, 48–67. [[CrossRef](#)]
56. Dietterich, T. Overfitting and undercomputing in machine learning. *ACM Comput. Surv. (CSUR)* **1995**, *27*, 326–327. [[CrossRef](#)]
57. Bejani, M.M.; Ghatte, M. A systematic review on overfitting control in shallow and deep neural networks. *Artif. Intell. Rev.* **2021**, *54*, 6391–6438. [[CrossRef](#)]
58. Baldo, N.; Miani, M.; Rondinella, F.; Celauro, C. Artificial Neural Network Prediction of Airport Pavement Moduli Using Interpolated Surface Deflection Data. In *IOP Conference Series: Materials Science and Engineering*; IOP Publishing: Bristol, UK, 2021; Volume 1203, p. 022112.
59. Alanazi, A.K.; Alizadeh, S.M.; Nurgalieva, K.S.; Nestic, S.; Grimaldo Guerrero, J.W.; Abo-Dief, H.M.; Eftekhari-Zadeh, E.; Nazemi, E.; Narozhnyy, I.M. Application of neural network and time-domain feature extraction techniques for determining volumetric percentages and the type of two phase flow regimes independent of scale layer thickness. *Appl. Sci.* **2022**, *12*, 1336. [[CrossRef](#)]
60. Baldo, N.; Miani, M.; Rondinella, F.; Celauro, C. A machine learning approach to determine airport asphalt concrete layer moduli using heavy weight deflectometer data. *Sustainability* **2021**, *13*, 8831. [[CrossRef](#)]
61. Lim, J.C.; Karakus, M.; Ozbakkaloglu, T. Evaluation of ultimate conditions of FRP-confined concrete columns using genetic programming. *Comput. Struct.* **2016**, *162*, 28–37. [[CrossRef](#)]
62. Roushangar, K.; Mouaze, D.; Shiri, J. Evaluation of genetic programming-based models for simulating friction factor in alluvial channels. *J. Hydrol.* **2014**, *517*, 1154–1161. [[CrossRef](#)]
63. Baldo, N.; Miani, M.; Rondinella, F.; Valentin, J.; Vackcová, P.; Manthos, E. Stiffness Data of High-Modulus Asphalt Concretes for Road Pavements: Predictive Modeling by Machine-Learning. *Coatings* **2022**, *12*, 54. [[CrossRef](#)]
64. Garson, D.G. Interpreting neural network connection weights. *AI Expert* **1991**, *6*, 47–51.
65. Moradi, M.J.; Hariri-Ardebili, M.A. Developing a library of shear walls database and the neural network based predictive meta-model. *Appl. Sci.* **2019**, *9*, 2562. [[CrossRef](#)]
66. Khorsandi, M.; Feghhi, S.; Salehizadeh, A.; Roshani, G. Developing a gamma ray fluid densitometer in petroleum products monitoring applications using Artificial Neural Network. *Radiat. Meas.* **2013**, *59*, 183–187. [[CrossRef](#)]
67. Blissett, R.; Rowson, N. A review of the multi-component utilisation of coal fly ash. *Fuel* **2012**, *97*, 1–23. [[CrossRef](#)]
68. Shehata, M.H.; Thomas, M.D. The effect of fly ash composition on the expansion of concrete due to alkali–silica reaction. *Cem. Concr. Res.* **2000**, *30*, 1063–1072. [[CrossRef](#)]
69. Ghanbari, M.; Hadian, A.; Nourbakhsh, A.; MacKenzie, K. Modeling and optimization of compressive strength and bulk density of metakaolin-based geopolymer using central composite design: A numerical and experimental study. *Ceram. Int.* **2017**, *43*, 324–335. [[CrossRef](#)]
70. Roshani, M.; Phan, G.; Faraj, R.H.; Phan, N.H.; Roshani, G.H.; Nazemi, B.; Corniani, E.; Nazemi, E. Proposing a gamma radiation based intelligent system for simultaneous analyzing and detecting type and amount of petroleum by-products. *Nucl. Eng. Technol.* **2021**, *53*, 1277–1283. [[CrossRef](#)]
71. Moradi, N.; Tavana, M.H.; Habibi, M.R.; Amiri, M.; Moradi, M.J.; Farhangi, V. Predicting the Compressive Strength of Concrete Containing Binary Supplementary Cementitious Material Using Machine Learning Approach. *Materials* **2022**, *15*, 5336. [[CrossRef](#)]
72. Berry, E.; Hemmings, R.; Cornelius, B. Mechanisms of hydration reactions in high volume fly ash pastes and mortars. *Cem. Concr. Compos.* **1990**, *12*, 253–261. [[CrossRef](#)]
73. Committee, A. *Building Code Requirements for Structural Concrete (ACI 318-08) and Commentary*; American Concrete Institute: Farmington Hills, MI, USA, 2008.
74. *BS 8110-1*; Structural Use of Concrete, Part 1—Code of Practice for Design and Construction. British Standards Institution: London, UK, 1997.

75. Sumer, M. Compressive strength and sulfate resistance properties of concretes containing Class F and Class C fly ashes. *Constr. Build. Mater.* **2012**, *34*, 531–536. [[CrossRef](#)]
76. Türkel, S. Long-term compressive strength and some other properties of controlled low strength materials made with pozzolanic cement and Class C fly ash. *J. Hazard. Mater.* **2006**, *137*, 261–266. [[CrossRef](#)]
77. Uysal, M.; Akyuncu, V. Durability performance of concrete incorporating Class F and Class C fly ashes. *Constr. Build. Mater.* **2012**, *34*, 170–178. [[CrossRef](#)]
78. Berry, E.; Malhotra, V.M. Fly ash for use in concrete—a critical review. *J. Proc.* **1980**, *77*, 59–73.
79. Leung, C.K.; Ng, M.Y.; Luk, H.C. Empirical approach for determining ultimate FRP strain in FRP-strengthened concrete beams. *J. Compos. Constr.* **2006**, *10*, 125–138. [[CrossRef](#)]